Department of Mechanical and
Industrial Engineering
University of Illinois at
Urbana-Champaign
Urbana, IL 61801

AFOSR-TR- 91 0249

RESEARCH EQUIPMENT PURCHASED UNDER DURIP GRANT AFOSR-89-0098

Prepared by:

Dr.. Herman Krier
Tel: (217) 333-0529

Prepared for:

Air Force Office of Scientific Research
Attn: Dr. Mitat A. Birkan, Program Manager
AFOSR/NA
Bolling Air Force Base
Washington, D.C. 20332-6448

March 1991

FINAL TECHNICAL REPORT

FINAL TECHNICAL REPORT

RESEARCH EQUIPMENT PURCHASED UNDER DURIP, GRANT AFOSR-89-0098

Prepared by:

Dr. Herman Krier
Principal Investigator
Department of Mechanical and Industrial Engineering
University of Illinois at Urbana-Champaign
(217) 333-0529

Prepared for:

Air Force Office of Scientific Research
Attn: Dr. Mitat A. Birkan, Program Manager
AFOSR/NA
Bolling Air Force Base
Washington, D.C. 20332-6448
(202) 767-4938

March 1991

A-1

REPORT DOCUMENTATION PAGE

1a REPORT SECURITY CLASSIFICATION: UNCLASSIFIED	1b RESTRICTIVE MARKINGS
2a SECURITY CLASSIFICATION AUTHORITY	3 DISTRIBUTION/AVAILABILITY OF REPORT: APPROVED FOR PUBLIC RELEASE; DISTRIBUTION IS UNLIMITED
2b DECLASSIFICATION/DOWNGRADING SCHEDULE	
4 PERFORMING ORGANIZATION REPORT NUMBER(S)	5 MONITORING ORGANIZATION REPORT NUMBER(S)
6a NAME OF PERFORMING ORGANIZATION: University of Illinois at Urbana-Champaign; 6b OFFICE SYMBOL (If applicable): UIUC	7a NAME OF MONITORING ORGANIZATION: AFOSR/NA
6c ADDRESS (City, State, and ZIP Code): Dept. of Mechanical & Industrial Engineering 138 MEB; 1206 West Green Street; MC-244 Urbana, Illinois 61801	7b ADDRESS (City, State, and ZIP Code): Building 410; Bolling Air Force Base Washington, D.C. 20332-6448
8a NAME OF FUNDING/SPONSORING ORGANIZATION: AFOSR/NA; 8b OFFICE SYMBOL (If applicable): NA	9 PROCUREMENT INSTRUMENT IDENTIFICATION NUMBER: AFOSR 89-0098
8c ADDRESS (City, State, and ZIP Code): Building 410; Bolling Air Force Base Washington, D.C. 20332-6448	10 SOURCE OF FUNDING NUMBERS: PROGRAM ELEMENT NO 61102F; PROJECT NO 2308; TASK NO A1; WORK UNIT ACCESSION NO

11 TITLE (Include Security Classification): RESEARCH EQUIPMENT PURCHASED UNDER DURIP GRANT NO. AFOSR 89-0098: APPLICATION FOR LASER PROPULSION

12 PERSONAL AUTHOR(S): Herman Krier

13a TYPE OF REPORT	13b TIME COVERED	14 DATE OF REPORT (Year, Month, Day)	15 PAGE COUNT
Final	FROM 09/89 TO 10/90	1991, March, 7	22

16 SUPPLEMENTARY NOTATION

17 COSATI CODES			18 SUBJECT TERMS (Continue on reverse if necessary and identify by block number)
FIELD	GROUP	SUB-GROUP	

19 ABSTRACT (Continue on reverse if necessary and identify by block number)

This report describes the research equipment purchased and how that equipment is being utilized to carry out research in the area of high temperature fluid mechanics and plasma dynamics resulting from laser supported plasmas. The development of the fundamental relationships that explain energy transport mechanisms in laser sustained plasmas require a wide range of experiments to be carried out. The equipment described in this document are a major component of the required experiments.

20 DISTRIBUTION/AVAILABILITY OF ABSTRACT	21 ABSTRACT SECURITY CLASSIFICATION
[X] UNCLASSIFIED/UNLIMITED [X] SAME AS RPT [X] DTIC USERS	UNCLASSIFIED
22a NAME OF RESPONSIBLE INDIVIDUAL: Dr. Mitat A. Birkan	22b TELEPHONE (Include Area Code): (202) 767-4938; 22c OFFICE SYMBOL: AFOSR/NA

DD FORM 1473, 84 MAR — 83 APR edition may be used until exhausted. All other editions are obsolete.

RESEARCH EQUIPMENT PURCHASED UNDER DURIP, GRANT AFOSR 89-0098

INTRODUCTION

Through AFOSR, as part of the Defense University Research Instrumentation Program the Department of Mechanical and Industrial Engineering of the University of Illinois was awarded the funds to purchase equipment in support of research dealing with high temperature thermodynamics, plasma formation, and laser gas interaction. AFOSR has been supporting research under a separate grant, a program dealing with Beamed Energy (Laser) Rocket Propulsion.

We requested and were awarded funds for a Duel Channel Infrared Imaging System described below. It's cost is $79,000:

Item I: Dual Channel Infrared Imaging System

(a) Description

The Inframetrics Model 610 High Performance Infrared Imaging Radiometer is a microprocessor-based duel channel system operating with a single operating path for simultaneous thermal imaging in both 3-5 μm and 8-12 μm spectral bands. The instrument allows quantitative and qualitative high resolution, non-intrusive temperature measurements. The capability to simultaneously analyze both long and short wave spectral bands allows the identification of thermal patterns within the target area.

(b) Specifications

- Spectral bandpass: 3-5 μm and 8-12 μm simultaneously
- Calibrated temperature range: 0-1500 degrees C.
- Able to capture thermal transients as short as 125 microseconds
- Quantitative temperature measurement of areas, points, and isotherms within the target area.
- Automatic emittance and background correction
- Minimum resolution element size: 30 μm (with auxiliary optics)
- 8:1 continuous zoom

(c) Costs

- Model 610 Dual Channel IR Imaging Radiometer	$71,500
- Auxiliary optics (for small targets)	
3x telescope	$ 6,900
6 inch close-up lens	$ 1,500
Total:	**$79,900**

(d) Manufacturer

Inframetrics
Attn: Andrew Teich
12 Oak Park Drive
Bedford, MA 01730
(617) 275-8990

I. ACTUAL EQUIPMENT PURCHASED

After a much more detailed investigation into the capabilities and performance specifications of the Inframetrics Dual Channel Radiometer, we reluctantly concluded that it was not well suited for meeting our laboratory diagnostic requirements.

As a temperature sensing device, the radiometer is much better suited for opaque targets than for participating gaseous media as in the plasma absorption chamber. Even though the device is capable of focusing on a specified plane in a gaseous volume, the results from such operation are not accurate, and require much post measurement analysis in order to derive a gas temperature. There are two reasons for this. First, emission from solid surfaces in front of or behind the gas must be taken into account after the measurement has been made, even though they are not in the plane of focus. Second, the emissivity and transmissivity of the participating media must be known as functions of temperature and wavelength. This information is available, but not very convenient to use, because it is temperature we are trying to determine. All of this means that additional measurements and calculations must be performed before a gas temperature can be determined, and the accuracy would not be very good. In addition, much of the device's sophisticated data reduction and instantaneous temperature display capabilities would be wasted in an applications such as this.

We then requested and were authorized by AFOSR to make the necessary changes in the equipment request to overcome the limitations of the original equipment. The capabilities of the permanent equipment purchased under the revised list completely encompassed the original equipment and allows to make state of the art high gas temperature measurements in a variety of ways.

All current evaluations of laser sustained plasma properties rely on the assumption of a circumferentially symmetric plasma and well characterized laser beam. The high power laser being used here at the University of Illinois College of Engineering has never been so characterized, and part of the equipment purchased will provide this service. The bulk of the remaining equipment was used to upgrade our laser induced fluorescence facilities, allowing us to make some of the most advanced LIF studies possible. Some equipment was also purchased that permitted highly accurate emission spectroscopic studies of the non-local thermodynamic equilibrium state of laser sustained hydrogen plasmas.

Table I is a summary of the permanent equipment purchased with this grant. The next section provides a more detailed description of the equipment, including the scientific impetus behind the purchases.

TABLE I: EQUIPMENT PURCHASED

No.	ITEM/DESCRIPTION	AMOUNT	P.O. #
1.	Laser Beam Diagnostics System (Spiricon Inc.)	28,780.00	JR98631
2.	LBD Host Computer (Arends & Sons Inc.)	6,925.00	JR97138
3.	LBD Mainframe Adapter (Wordlink)	276.00	JRD4262
4.	LBD Mainframe Adapter Cable (Cabletron)	302.58	JRD 4261
5.	LBD ZnSe Beamsteering Optics (Janos Inc.)	9,887.00	JR13448
6.	LBD Optical Mounts (Oriel Corp.)	869.74 298.49	JR19192 JRD4256
7.	Intelligent Laser Controller (Lambda Physik)	8,544.00	JR98521
8.	ILC Pressure Sensor Fitting (Peoria Valve)	10.96	JRD4257
9.	Excimer Laser Halogen Filter (Lambda Physik)	92.31	JRD4263
10.	Photomultiplier Tube (Hamamatsu Corp.)	1,004.00	JR97796
11.	Digital Oscilloscope (Hewlett Packard)	2,772.00	JR10851
12.	Dye Laser Grating (Lambda Physik)	2,772.90	JR87296
13.	Dye Laser Beam Expander	310.00	JRD 1122
14.	Laser Frequency Doubler (Lumonics)	7,272.95	JR97038
15.	Image Quality Bandpass Filters (Andover)	3,092.95	JR97020
16.	Infrared Detector (Cincinnati Electronics)	4,997.05	JR80799
17.	Hydrogen Safe Gas Regulator (Depke)	884.00	JR26413
18.	Concave Mirror (Oriel Corp.)	314.00	JRD4731
19.	Mirror Mount (Aerotech)	490.00	JRD4732

Total = **$ 79,895.93**

II. DESCRIPTION AND JUSTIFICATION OF PURCHASES

Item numbers from Table I

1. Laser Beam Diagnostics System

This equipment is needed in order to obtain accurate laser beam profile data and to assure the highest quality beam possible. The acquisition of meaningful spectroscopic data for the purpose of high gas temperature measurements depends directly upon this piece of equipment.

2-6. Laser Beam Diagnostics System; peripheral components

These components are required for the optimal operation of the LBD system in our laboratory. A host computer is required for the acquisition and initial processing of the beam profile data, with a hookup to an ethernet line for further mainframe processing. Due to the high power in our CW CO_2 laser beam, special ZnSe beamsteering optics are required for directing a portion of the beam into the LBD system. These optics must be properly mounted within our laboratory work space.

7-9. Intelligent Laser Controller

This piece of equipment is needed for the implementation of laser induced fluorescence studies in our laboratory. With it pulse energy is stabilized over long periods of time without the need for frequent, time consuming, and expensive excimer laser gas changeovers. This system requires a laser gas reservoir pressure sensor for which a fitting had to be purchased separately. The halogen filters are required for effective pumping of the laser chamber resulting in the highest possible output pulse energy.

10-11. Fluorescence Studies Equipment

These two pieces of equipment are required for the operation of the Boxcar integrator purchased with an earlier URIP. The PMT is needed to measure the signal processed by the Boxcar, and the high speed oscilloscope is needed to facilitate experiment timing schemes.

12-13. Fluorescence Studies Equipment

These items are required for the reliable undertaking of the laser induced fluorescence studies aimed at measuring high gas temperatures. The dye laser grating installed permits high efficiency laser coupling and tunability. The beam expander is needed for output manipulation prior to entering the gas chamber.

14-15. Fluorescence Studies Equipment

These items are also needed for laser induced fluorescence work. The frequency doubler permits the fluorescent probing of gas species out of the normal frequency range of the tunable dye laser. The image quality bandpass filters are used for isolating the output fluorescence signal for data processing.

16. Infrared Detector

This detector is central to the radiation temperature measurement of flowing particles.

17. Hydrogen Safe Gas Regulator

This regulator is required to the extension of our hydrogen gas plasma experiments to the necessary flow rates.

18-19. Self-Absorption Correction

These items are required for the correction of plasma spectral emission self-absorption in the plasma volume. This correction is key to the accurate determination of non-equilibrium parameters within the plasma.

tup:
ta taken: Fri Jul 20 09:41:16 1990

tolog Time Period=1 sec Gain=10 Phase=180 Samples=4 Gain Corrected YES

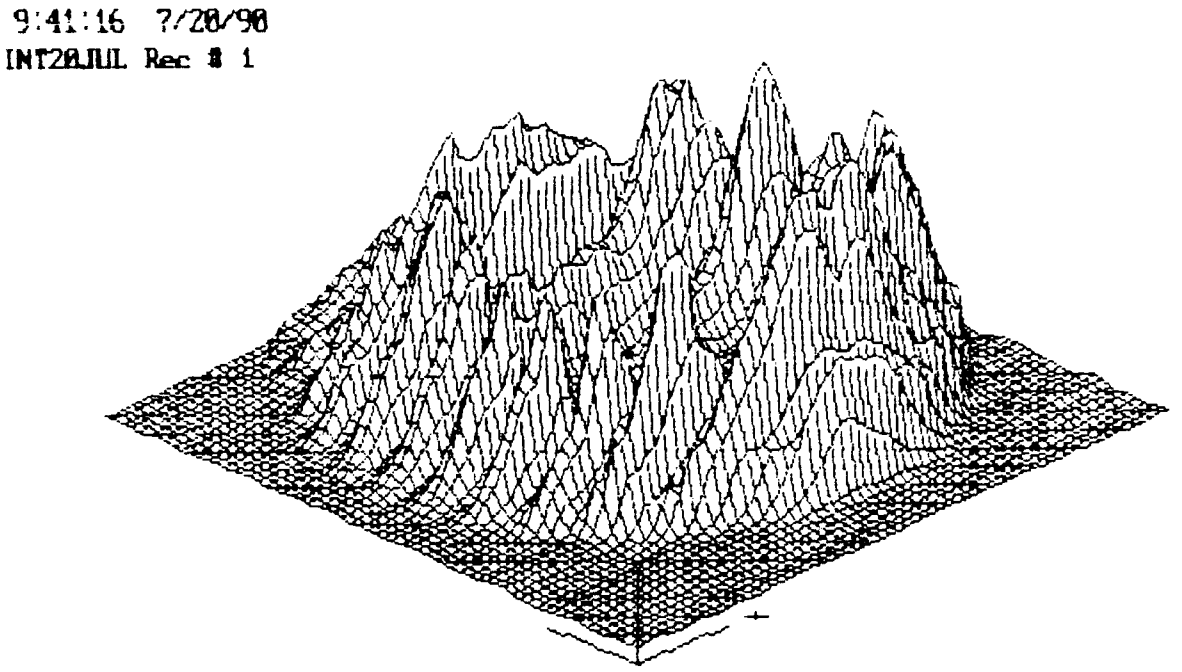

splayed as follows:
tation=45 Tilt=30 Slice=2 Format=HX Sec Data=NONE
area displayed = 1 to 127, Y area displayed = 3 to 127

antitative Measurements:
mputations made using 1.00% of Peak method

m=45.4500 mm Energy=7014584.0000 Peak/Aver=5.9516
anX=72.0794 MeanY=69.7260 PeakX=77 PeakY=27
us X= 0.0000 Gaus Y= 0.0000 Gaus Height= 0.0000
  Wx= 0.0000mm Wy= 0.0000mm Coeff= 0.0000
l Diameter=0.0000 Cyl Height=0.0000 Cyl Coeff=0.0000
p Hat Dia=0.0000 Top Hat Height=0.0000 Top Hat Std Dev=0.0000

nted using SPIRICON LOOD Software Package Mon Oct 29 18:06:05 1990

Figure 1.

tup:
ta taken: Mon May 14 10:09:30 1990

tolog Time Period=1 sec Gain=10 Phase=180 Samples=4 Gain Corrected (E

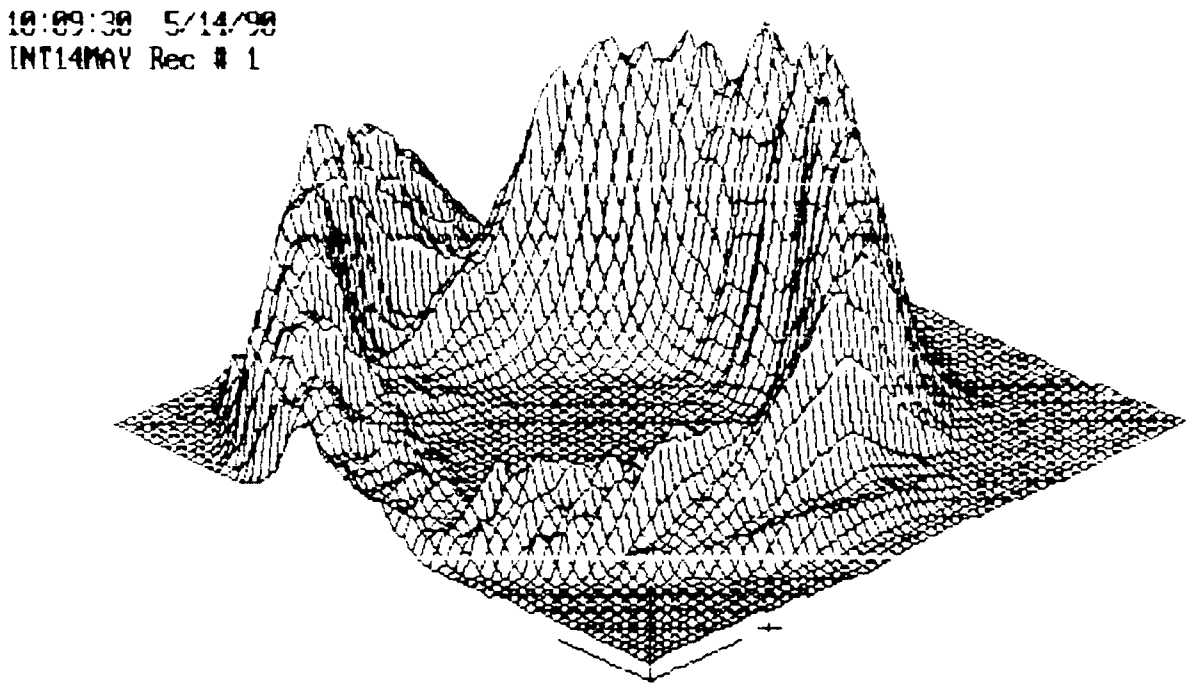

splayed as follows:
tation=45 Tilt=30 Slice=2 Format=Hx Sec Data=NONE
area displayed = 1 to 127, Y area displayed = 1 to 127

antitative Measurements:
mputations made using 1.00% of Peak method

am=46.5571 mm Energy=887988.0000 Peak/Aver=5.3908
ms=6c.7815 Meanx=74.8594 Peakx=95 PeakY=57
Gaus X= 0.0000 Gaus Y= 0.0000 Gaus Height= 0.0000
Wx= 0.0000mm Wy= 0.0000mm Coeff= 0.0000
l Diameter=0.0000 Cyl Height=0.0000 Cyl Coeff=0.0000
p Hat Dia=0.0000 Top Hat Height=0.0000 Top Hat Std Dev=0.0000

inted using SPIRICON OOID Software Package Mon Oct 29 16:01:06 1990

Figure 2.

III Use of Beta-Barium Borate Frequency Doubling Crystal/Compensator and Bandpass Filters in Compressible Mixing Layer Research

The newly acquired beta-barium borate (BBB) crystal and compensator (Lumonics) will be integral to the success of a study of compressible mixing layers at the University of Illinois at Urbana. Planar laser-induced fluorescence measurements of the species concentration and temperature transport across both reactive and nonreactive two-dimensional planar free shear layers are being conducted in an effort to study compressible entrainment and mixing. The new crystal is being used to supplement the existing doubling crystal originally bought with the dye laser. Unfortunately, the original crystal had a doubling range limited from 282 nm to 330 nm, which is well suited to excitation of OH in reactive flows but is useless for nonreactive studies. The nonreactive studies require the injection of a suitable seed molecule, a prime candidate being nitric oxide (NO). The (0,0) band of NO lies near 225 nm, far out of the range of the original doubling crystal. Alternative crystals are available, however they were rather impractical due to their extremely low efficiency at the low ultraviolet wavelengths necessary for pumping NO. Another advantage of the BBB crystal is its extended range of operation out to approximately 300 nm, thereby enabling higher efficiency pumping of OH(1,0) transitions than the original crystal.

Collection of the fluorescence data is also important to the ultimate analysis of the data. Bandpass filters are to be used to collect selected vibrational bands, which simplifies modelling of the transition processes to yield more accurate temperature and specie concentration measurements of the mixing layer. The custom bandpass filter at 235 nm will be used to collect the strong emission from the (0,1) vibrational band of NO, while the other filters are of use in isolating the (0,0) and (1,1) vibrational bands of OH. Laser-induced fluorescence of NO can be used in both reactive and nonreactive mixing flows, enabling temperature and concentration measurements at all flow conditions, while these data can be supplemented by OH fluorescence in the reactive cases.

This equipment is vital to the successful application of laser-induced fluorescence in the experimental study of compressible mixing layers. The resultant data is expected to fill an existing gap in the understanding of entrainment and mixedness by compiling the probability density functions of passive scalars (density, temperature and species concentration) across the shear layer. Information of this type is lacking in compressible mixing layers and must be measured if chemical modelling of supersonic combustion is to be put on a sound physical basis. It must also be mentioned that use of this equipment is

not restricted to these particular conditions, flowfield and study. Other research groups, particularly those involved with combustion, may find a need for a frequency doubled dye laser output within the range of the new crystal.

IV. SINGLE PARTICLE OPTICAL DIAGNOSTICS

A. Particle Temperature

The temperature of the particles are measured using a two-color pyrometer. A schematic of the system can be seen in Fig. 3. The burning particles are first imaged on an aperture which limits the sampling volume inside the reactor. This is done with a 1:1 magnification mirror system consisting of a primary concave spherical mirror and a secondary convex spherical mirror. The particles are then imaged on two liquid nitrogen cooled Indium Antimonide (InSb) Infrared detectors using a collimating mirror, beamsplitter and two focusing lenses. Infrared wavelengths were chosen to reduce absorption by the soot cloud surrounding the particle which has theoretically been shown to effect the temperature measurement. The detectors are filtered at wavelengths of 1.47-1.86 and 2.00-2.34 μm with filters mounted inside to reduce noise. The ratio of these signals is used to calculate temperature using Planck's radiation law and assuming the particles are gray bodies. The validity of the assumption of gray behavior of carbon particles has been justified by others through experimental studies.

The calibration was performed using a blackbody radiation source of known temperature. The coal particles are simulated with pinholes mounted on a spinning disc backlit with the blackbody source. The temperature measurements have been shown to be insensitive to variations in particle size and velocity. The data points are fit using Planck's law integrated over the known transmission regions of each filter. A schematic of the calibration setup is shown in Fig. 4.

B. Particle Imaging

Images of the nonspherical burning particles are optioned in one of two ways: (1) using a digital camera, and (2) using a 35 mm camera. The digital camera consists of a 128x128 photodiode array which allows the user to view the images as they are taken. This is essential when lining up the system or when high data collection rates are necessary. The 35 mm camera is used when higher resolution is desired. In either case, a pulsed light source is used to illuminate and effectively "freeze" the particle at very high

velocities. A long working distance microscope lens is used to magnify the particle image by as much as 35x allowing great detail to be observed. The components of the imaging system can be seen with the two-color pyrometer in Fig. 3. The 35 mm prints can also be digitized which enables size/shape information to be obtained quantitatively for either case.

C. Particle Velocity

Particle velocity is measured using a transit timing technique with the trigger system and the two-color pyrometer. The trigger consists of a series of lenses focused on a phototransistor which is activated when a burning particle passes through its focal volume inside the reactor. This focal volume will be located above the focal volume of the pyrometer, and by knowing what distance the velocity is calculated by recording the time between the successive signals. The trigger can also be seen in Fig. 3.

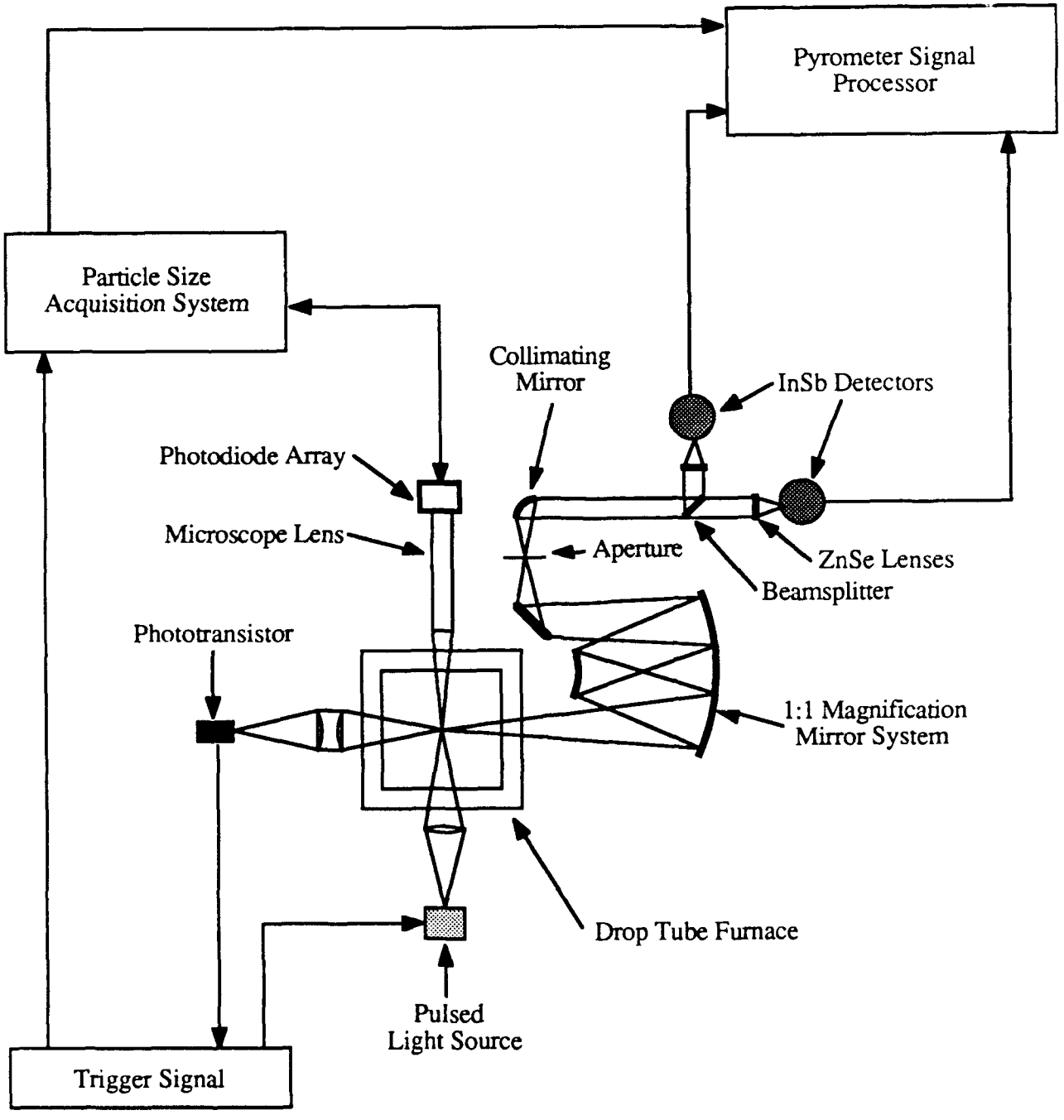

Optical diagnostics used to simultaneously measure size, temperature and velocity of individual particles.

Figure 3.

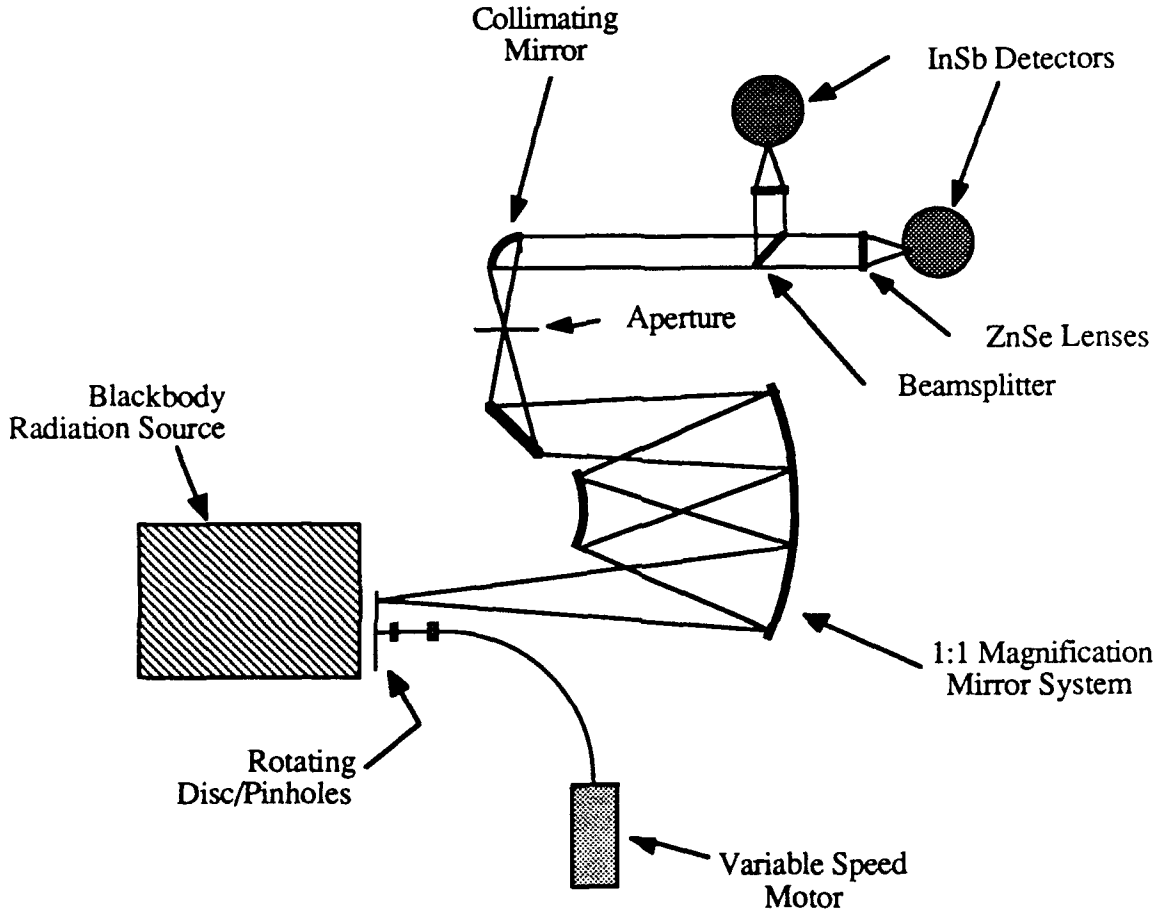

Calibration of Two-Color pyrometer using moving pinhole backlit with blackbody radiation source.

Figure 4.

Appendix A

The following is a paper presented at the AIAA/DGLR/JSASS 21st International Electric Propulsion Conference, July 18-20, 1990. It contains results obtained using some of the equipment purchased on this grant, in particular the hydrogen safety related items.

AIAA 90-2637

Continuous Wave Laser Sustained Hydrogen Plasmas for Thermal Rocket Propulsion

A. Mertogul, D. Zerkle, H. Krier, and J. Mazumder

University of Illinois at Urbana-Champaign
Urbana, Illinois

AIAA/DGLR/JSASS
21st International Electric Propulsion Conference
July 18-20, 1990 / Orlando, FL

CONTINUOUS WAVE LASER SUSTAINED HYDROGEN PLASMAS FOR THERMAL ROCKET PROPULSION†

A. Mertogul*, D. Zerkle*, H. Krier‡, J. Mazumder**

University of Illinois at Urbana-Champaign
Department of Mechanical and Industrial Engineering
Urbana, Illinois

Abstract

Results of continuous wave laser sustained plasmas (LSP's) in flowing hydrogen with application to thermal rocket propulsion are reported. The key measured figures of merit are plasma global absorption and thermal efficiency. The range of conditions studied include gas pressures from 1.77 atm to 4.09 atm, input laser power from 3.25 kW to 7 kW, f/4 and f/7 beam focusing geometries, and H_2 mole fluxes from approximately 600 moles/m^{2}s to 2355 moles/m^{2}s. Global absorption is found to be a strong function of both laser power and gas pressure, but remains nearly constant versus changes in mole flux. Thermal efficiency is a function of laser power, gas pressure and mole flux, with higher powers and pressures resulting in higher optimum mole fluxes. The maximum recorded values for global absorption and thermal efficiency are 89.8% and 80.2% respectively. Hydrogen LSP thermal efficiency of 80% far surpasses the previous best argon LSP thermal efficiency of 58%, and validates the conclusion that laser sustained hydrogen plasma thrusters are feasible.

Introduction

Laser propulsion is an orbital transfer technology based on the use of a remote laser as the power source. In such a system energy from the laser would be converted to propellant thermal energy within a spacecraft absorption chamber via a laser sustained plasma (LSP). The LSP would absorb a major portion of the incident beam (ideally 100%) and the propellant gas flowing through the absorption chamber would be heated via conduction and convection from the plasma. Assuming a large fraction of the incident laser energy is converted to propellant thermal energy, the propellant could be exhausted through a nozzle to produce thrust.

The feasibility of laser propulsion is contingent upon a large fraction of the incident laser power being converted to propellant thermal energy. This conversion of energy by the LSP can be viewed as a two step process. The incident energy must first be absorbed by the LSP (primarily through inverse Bremsstrahlung). The fraction of the incident energy that is absorbed is defined as the global absorption. The second step is the transfer of energy from the extremely hot LSP to the flowing propellant gas. The fraction of incident energy retained by the propellant gas as thermal energy is defined as the thermal efficiency.

It is known that the LSP will occupy a position in the focusing beam where power absorbed from the laser is balanced by power lost by conduction, convection, and radiation [1,2]. Ideally a large portion of the absorbed energy is transported to the flowing propellant by conduction and convection, and a relatively small portion lost due to optically thin radiation. By varying the conditions under which the LSP is operated, these proportions are controlled to achieve optimum thermal efficiency.

The position of the LSP changes to accommodate changes in operating conditions and maintain an energy balance. However if the mole flux is too great or if the power or gas pressure are decreased significantly, more energy is lost than absorbed by the LSP, and the LSP becomes unstable and extinguishes. This phenomenon is commonly referred to as blowout. The focus of this and previous experimental work at the University of Illinois at Urbana-Champaign (UIUC) is to measure global absorption and thermal efficiency versus variations in the four control parameters - gas pressure, gas mole flux, laser power, and incident beam focusing geometry.

If a full scale laser propulsion system proves feasible, it will have advantages over both conventional chemical and electric propulsion technologies. Typically chemical rockets produce exceedingly high thrusts but low specific impulses of 250 to 480 s. Electric propulsion systems achieve specific impulses of 4000 s and greater but are typically limited by the amount of thrust produced. A laser thruster could fill the performance gap between these two technologies.

Because no combustible fuel is required, the type of propellant used by a laser thruster is chosen to optimize performance. Ideally hydrogen would be used because of its lowest molecular weight. A remote power source eliminates extra weight and results in a lightweight spacecraft with power limited only by the power of the source laser. The simple equation relating thrust and specific impulse is,

$$F = \frac{2\,\eta_{comb}\,P_{laser}}{I_{sp}\,g_o} \qquad (1)$$

where η_{comb} is the combined thermal and nozzle efficiencies, P_{laser} is the incident laser power, I_{sp} is the specific impulse, and g_o is the gravitation constant. Assuming a nozzle efficiency (conversion of thermal energy to propellant kinetic energy) close to unity, η_{comb} could simply be replaced by the thermal efficiency, η. It is clear from Fig. 1 that a 10 MW laser thruster with 1000 seconds specific impulse could produce well over 1 kN of thrust at a combined efficiency of 75%.

Continuous wave LSP's in a forced convective flow have been studied experimentally over the past seven years both at the UIUC and at the University of Tennessee

---

* Graduate Research Assistant, Student Member AIAA
‡ Professor, Fellow AIAA
** Professor, Member AIAA

† This research is supported by the US Air Force Office of Scientific Research under grant AFOSR 89-0274; Dr. Mitat Birkan is Program Manager.

Space Institute (UTSI). Keefer and co-workers at UTSI have studied argon LSP's at less than 1 kW input laser power, up to 4.5 m/s gas flow velocity, up to 4 atm gas pressure, and several beam geometries [1,3]. Their results include global absorption as high as 86% and thermal efficiency of 38% for a 2.5 atm argon LSP. Work done by Krier, Mazumder, and colleagues at UIUC, using single argon LSP's has produced global absorption as high as 97% and thermal efficiency as high as 46% at 2.5 atm gas pressure [2].

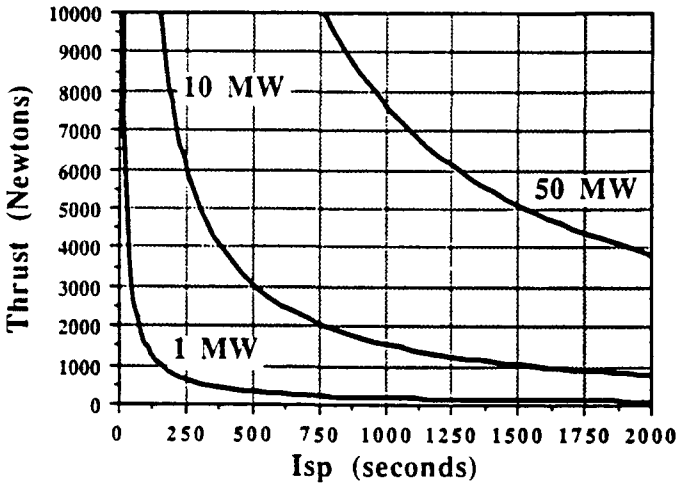

Figure 1 Relation between thrust and specific impulse for a laser thruster with 75% combined efficiency.

Having exhausted the possibilities for single argon plasmas, work at UIUC turned to dual (two plasmas side by side) LSP's with variable focal separation distance. The dual LSP work produced thermal efficiencies as nigh as 58% and showed that there was a slight advantage of using dual LSP's each at a given power over a single LSP at that power [4]. All of this previous work was done using argon as the propellant gas even though hydrogen is clearly the propellant of choice. Argon was used because it was inexpensive, non-toxic, readily available, and did not require any specialized safety equipment. Just as important, argon is similar to hydrogen in its absorptive and radiative properties. The work reported below represents the first study of global absorption and thermal efficiency conducted using hydrogen as the propellant gas.

Experimental Facility

An Avco-Everett 10 kW continuous wave CO_2 laser is the power source used to initiate and sustain the LSP's in this work. The laser output is a horizontal annulus approximately 50 mm i.d. and 75 mm o.d. The horizontal beam is turned vertically underneath the flow chamber with three water-cooled copper turning mirrors. A vertically translatable plano-convex zinc selenide (ZnSe) lens is positioned to focus the beam through a ZnSe sealing window into a stainless steel flow chamber. The f-number of the incident beam is changed by simply changing the focusing lens. Two lenses, of 300 mm and 530 mm focal length, are used in this study. A schematic representation of the test stand is shown in Fig. 2.

Initiation of a plasma is achieved by focusing the incident beam onto a tungsten rod which has been ground flat. The tungsten rod releases electrons through thermionic emission when struck by the laser beam. These electrons in the presence of the flowing propellant absorb laser energy through inverse Bremsstrahlung [5]. The gas is thus heated and breakdown of the gas is achieved. Once the plasma has been initiated the tungsten rod is retracted from the flow. The entire initiation procedure requires only a fraction of a second.

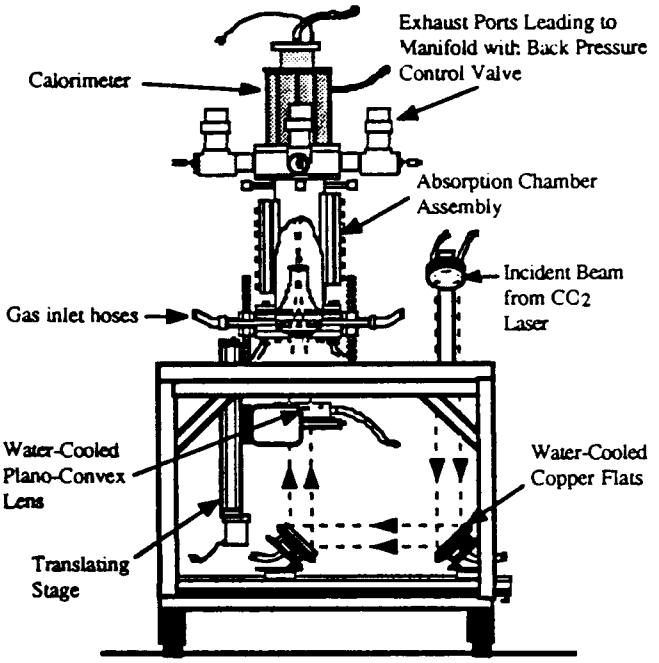

Figure 2 Schematic representation of LSP test stand.

The focal spot size of the laser is measured using short duration low power bursts from the laser to burn holes through thin Plexiglass sheets. Measurement of these holes yielded an estimate of focal spot diameter of 1 mm. This estimate is thought to be high due to melting and expansion of the test Plexiglass. Another estimate of focal spot diameter based on ray tracing to include spherical aberration and diffraction effects is 0.2 mm. Based on 7000 Watts incident power and a 0.2 mm focal diameter, the focal power flux is approximately 10^7 Watts/cm^2.

The propellant gas is introduced radially into the bottom of the flow chamber through a sintered steel flow straightener to diminish inlet turbulence, and accelerated with a 48 mm terminal i.d. converging quartz tube. Laser energy not absorbed by the plasma is collected by a water-cooled copper cone calorimeter bolted to the top of the flow chamber. Measurement of this transmitted energy is used to calculate LSP global absorption.

Exhaust gas temperatures are measured by millisecond response, type K thermocouples in each of four 2-inch insulated exit ports. The four exhaust gas temperatures are averaged and compared with the measured gas inlet temperature for the calculation of plasma thermal efficiency. The four exhaust pipes are manifolded into a single pipe that is valved for chamber pressure control. A detailed schematic of the absorption chamber assembly is shown in Fig. 3.

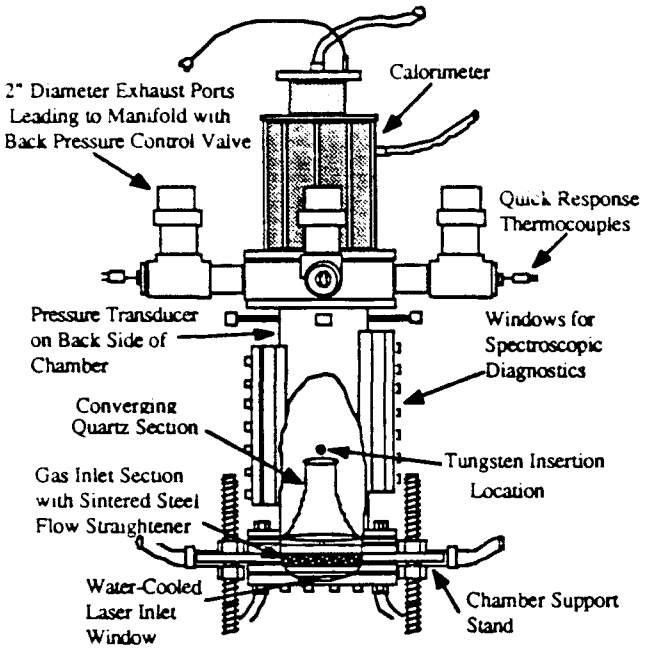

Figure 3 Detailed schematic of absorption chamber assembly.

In order to allow the safe use of hydrogen a new safety system had to be designed and installed. The main feature of the system is an exhaust hood positioned directly over the absorption chamber. A central control console is used to control chamber pressure through a microprocessor controller as well as to monitor five strategically positioned hydrogen detectors. In the case of a system trip, whether due to a leak or over-pressurization of the absorption chamber, the laser is automatically shut off. In addition the hydrogen flow is shut off and an argon purge supply is activated through the use of automatic pneumatically actuated valves. The system can also be tripped manually if necessary.

Data Analysis

Temperatures, chamber pressure, and calorimeter data from experiments are scanned and recorded once per second for use in data reduction. Eight consecutive scans are averaged for every reduced data point in order to smooth random fluctuations in the data. LSP global absorption is defined as the fraction of the incident laser power absorbed by the plasma. Plasma absorption measurements are made indirectly using a calibrated water-cooled copper cone calorimeter.

Measurement error analysis is performed following Kline and McClintock [6]. Errors associated with calorimeter measurements are grouped as those caused by errors in the calibration, those caused by heated gas within the chamber exchanging heat with the calorimeter, and those caused by scattering of the laser radiation and plasma irradiation of the calorimeter. The calorimeter is calibrated by irradiating it with a known amount of laser power and measuring its response. Therefore the only errors in the calorimeter calibration are the input laser power uncertainty of ±3% and the cooling water mass flow of approximately ±4%. Errors due to gas heating are known to be less than 3% in experiments involving argon [7]. The error due to gas heating biases the data by causing artificially high transmitted power measurements which result in artificially low values for absorption. Errors due to laser scattering and plasma irradiation were assumed to be negligible.

Accounting for all sources of error, a good estimate for the total calorimeter incident power measurement absolute error is ±5% per measurement. This transmitted power measurement is then used in equation 2 to determine global absorption with an absolute error of ±1%.

$$\alpha = \frac{P_{laser} - P_{transmitted}}{P_{laser}} \qquad (2)$$

The thermal efficiency of the LSP is defined as the fraction of incident laser power retained by the working gas as thermal power. This quantity is determined by the change in the gas enthalpy (ΔH), using

$$\Delta \dot{H} = \dot{m} C_p (T_e - T_i) \qquad (3)$$

where $\dot{m}$ is the measured mass flow rate, C_p is the specific heat of the gas, T_e is the mass averaged exhaust gas stagnation temperature, and T_i is the mass averaged inlet gas stagnation temperature. The efficiency is then determined by the ratio of $\Delta \dot{H}$ to the laser power input to the plasma.

Errors involved in the calculation of thermal efficiency include ±3% for the gas mass flow, ±3% for the incident laser power, and ±1% for each thermocouple. Energy lost to the chamber walls before the heated gas reaches the thermocouples also contributes to the error, but is difficult to quantify. The error due to this heat loss is small after the chamber walls have been allowed to heat up to a sufficiently steady state. At this condition the heat loss is restricted to free convection from the outside of the chamber to the room air, and is small. Thermal efficiency is determined by equation 4 with an absolute error of ±5%.

$$\eta = \frac{\Delta \dot{H}}{P_{laser}} \qquad (4)$$

Experimental Results

The global absorption and thermal efficiency for hydrogen LSP's will be presented in four sections, each section representing the effect of the variation of one control parameter. Input laser power is considered first.

The global absorption of a hydrogen LSP is found to be strongly influenced by the laser input power. It is evident from the plots in Figs. 4 and 5 that global absorption increases with laser power. It is apparent from the data in Fig. 4 that for a given gas pressure, global absorption is determined by the input power and is relatively independent of the mole flux. In addition the limit of LSP stability (or blowout limit as it is often called) increases with input power. Note that at 3.5 kW no plasmas could be held stable at mole fluxes beyond approximately 2000 moles/m^{2}s. None of the 5 or 7 kW LSP's were made to become unstable at this pressure at the mole fluxes presented.

For reference purposes, 2000 moles/m^{2}s of hydrogen is 7.3 g/m^{2}s which at 3.5 atm corresponds to 13.7 m/s average flow speed prior to impinging on the LSP. The flow tube is 48 mm in diameter.

Although for a given mole flux and gas pressure greater absorption is achieved at greater power, the LSP thermal efficiency does not follow such a simple relation. For a given mole flux and pressure, the thermal efficiency

of the LSP depends on how close the conditions are to the optimal mole flux. Although mole flux effects will be discussed in a later section, it can briefly be stated that for a given pressure an increase in power corresponds to an increase in optimal mole flux. Referring to the plot in Fig. 5, the thermal efficiency first increases with input power before decreasing . This is because the difference between the optimal mole flux and the mole flux given in the plot first decreases and then increases with input power going from 3.25 to 7 kW.

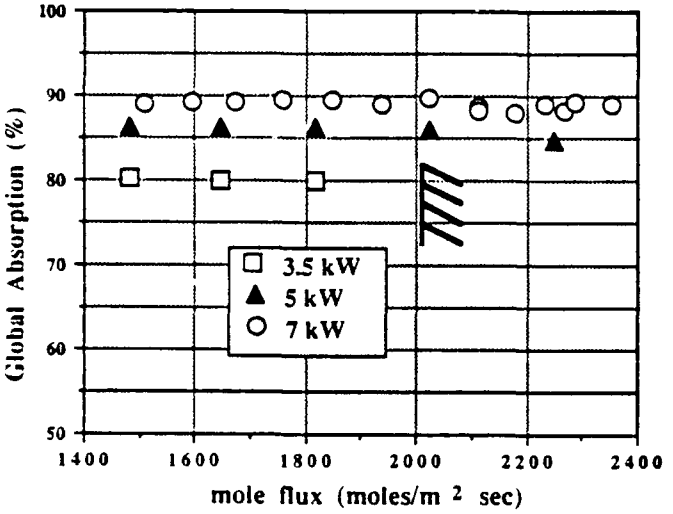

Figure 4 Comparison of global absorption with varying input laser power for 3.5, 5, and 7 kW LSP's at 3.53±0.11 atm with f/4 focusing geometry. The symbol resembling a wall at 2023 moles/m²s indicates mole flux stability limit for 3.5 kW LSP's.

It is clear from the previous discussion that since higher power results in higher absorptions and a greater stability limit, greater thermal efficiencies are possible at higher powers and mole fluxes which are beyond the stability limit at low powers.

Varying gas pressure affects global absorption and thermal efficiency similarly to varying laser power. The stability of LSP's is very strongly influenced by gas pressure. At 7 kW input power, and f/4 focusing geometry, LSP's at 1.80 atm are not stable beyond 1011 moles/m²s. However at the same conditions and 3.53 atm, the LSP's exhibit no instabilities and are stable at mole fluxes as high as 2355 moles/m²s. Similarly LSP's at 5 kW, f/4, 2.14 atm are not stable at mole fluxes greater than 1075 moles/m²s, but at the same conditions and 3.53 atm the LSP's again exhibit no instabilities and are stable at mole fluxes as high as 2247 moles/m²s.

Increases in gas pressure also result in increases in global absorption, although the absorption increase appears to level off at the highest pressures considered, 3.53 and 4.08 atm, as indicated by the plot in Fig. 6. As is the case with increasing input power, increasing the gas pressure causes an increase in the optimal mole flux. As is evident from the previous discussion and the data in Fig. 6, increased global absorption from increased gas pressure allows for the possibility of increased thermal efficiency if the mole flux can be optimized.

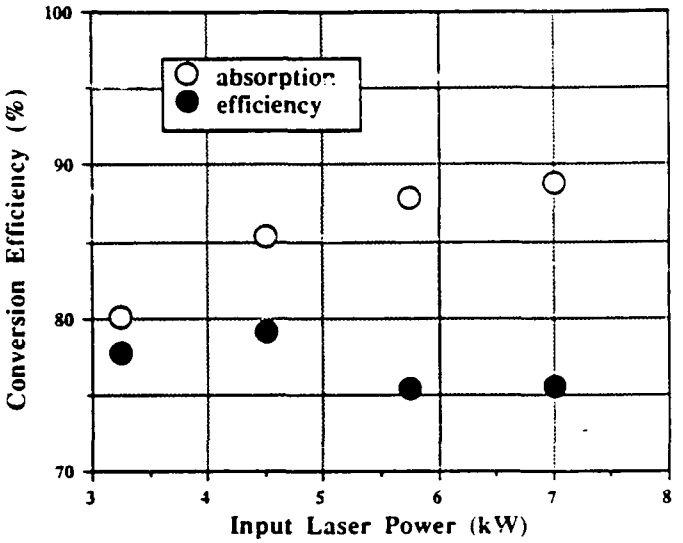

Figure 5 Global absorption and thermal efficiency for a series of LSP's at 4.07 ± 0.02 atm, 1982 moles/m²s, f/4, 3.25 to 7 kW input power.

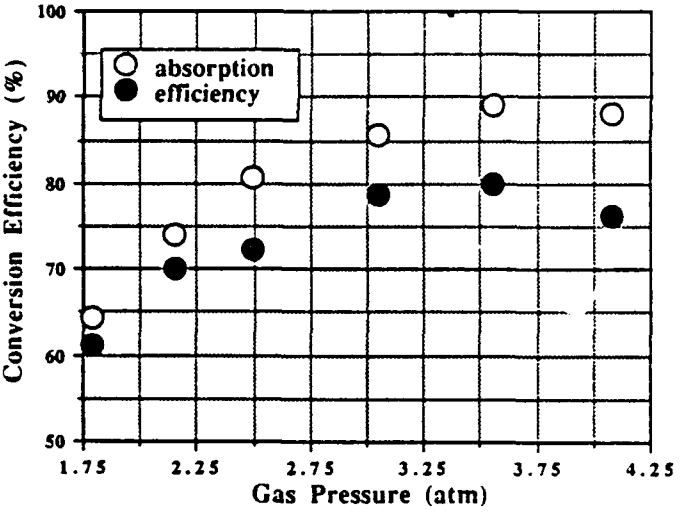

Figure 6 Comparison of maximum recorded thermal efficiency and corresponding global absorption for 7 kW, f/4 LSP's at the indicated pressures. Thermal efficiencies at 2.49 and 4.08 atm were not at optimal mole flux and therefore appear low.

In order to observe the effects of varying focusing geometry, 7 kW, f/7 LSP experiments were done at 2.52, 3.05, and 3.54 atm for comparison with 7 kW, f/4 experiments at those pressures. In all cases f/7 LSP's produce lower global absorption and lower thermal efficiency than f/4 LSP's. A comparison of f/4 and f/7 LSP performance is shown in Fig. 7. In addition it is observed that the f/4 geometry produces LSP's which are stable at higher mole fluxes than the f/7 geometry. At

7 kW input power, and f/7 focusing geometry, LSP's at 1.84 atm are not stable beyond 882 moles/m^{2}s. Previously it was noted that at 1.80 atm, f/4, 7 kW LSP's are not stable beyond 1011 moles/m^{2}s.

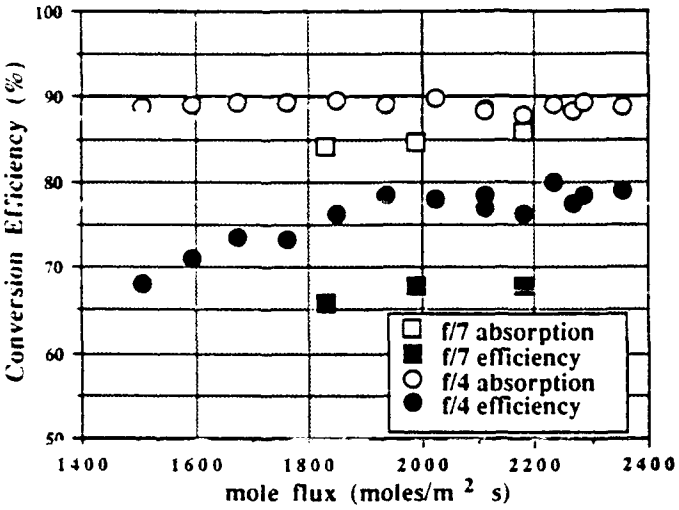

Figure 7 Comparison of global absorption and thermal efficiency of 7 kW, f/4 LSP's at 3.53 ± 0.11 atm, and 7 kW, f/7 LSP's at 3.54 ± 0.02 atm.

The effect of varying mole flux was briefly touched upon above. It is important to have a physical understanding of what the variation of mole flux does to LSP behavior. A stable LSP exists in a state of balance where energy in equals energy out. An increase in the mole flux results in an increase in the LSP convective transfer to the propellant and causes the LSP to shift downstream (closer to the focus) to a position in the focused beam with a higher power flux. The LSP restabilizes at a point where the energy absorbed balances the increased energy loss. However if the beam power is insufficient, the LSP is pushed past the focus where it extinguishes.

Following this reasoning it is apparent why the mole flux for optimum thermal efficiency increases with increases in both laser power and gas pressure. An increase in laser power causes an increase in power flux and results in the LSP repositioning upstream where the input power flux again balances losses. Similarly an increase in gas pressure increases the local absorption coefficient (due to an overall increase in electron number density) causing the LSP to again travel upstream to a beam position with a lower flux where the energy balance is reestablished. Optimally the LSP is positioned where the losses to the propellant (convective and conductive) are maximized. This optimization is achieved for a given input power, gas pressure, and focusing geometry by an increase in the mole flux as long as the LSP remains stable.

Because increases in both laser power and gas pressure cause the LSP to shift upstream, both increases require higher mole fluxes to push the LSP back downstream to the optimal position. This behavior is indicated by the plots in Figs. 8 and 9.

Referring to the data in Fig. 8, the optimum mole flux at 3.5 kW occurs at 1645 moles/m^{2}s. LSP instability follows soon after at 2023 moles/m^{2}s. The 5 kW LSP's appear to optimize at 2023 moles/m^{2}s, and although there is some scatter the 7 kW LSP's appear to optimize near 2231 moles/m^{2}s. This data illustrates the need for higher mole fluxes to optimize higher power LSP's (that is, 10 MW).

Referring to the data in Fig. 9, the thermal efficiency appears to peak at 1949 moles/m^{2}s for the 3.03 atm LSP's, and near 2231 moles/m^{2}s for the 3.53 atm LSP's. This data illustrates the need for higher mole fluxes to optimize higher pressure LSP's. This data also illustrates the classic behavior of thermal efficiency versus mole flux which involves a steady increase followed by a decrease and then instability. Although the 3.53 atm data does not show a true peak the point at 2231 moles/m^{2}s has been used as the optimum for comparisons. Although no instabilities are apparent, it is believed that the highest mole fluxes shown are near the instability threshold.

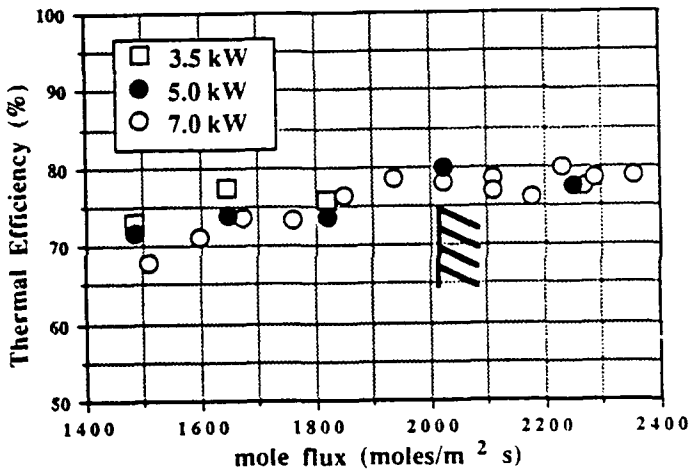

Figure 8 Comparison of thermal efficiency plotted versus mole flux for f/4, 3.5, 5.0, and 7.0 kW LSP's at 3.53±0.11 atm gas pressure. The symbol resembling a wall represents 3.5 kW mole flux stability limit.

Mole flux has a small effect on global absorption as is indicated by the plot in Fig. 4. In some cases there does appear to be a slight decrease in absorption with increasing mole flux at mole fluxes well below optimum. However at the mole fluxes of interest (those near optimum thermal efficiency) global absorption has little variation. Although not evidenced in the data shown here, it is possible for global absorption to decrease at very high mole flux. This was shown to occur in argon LSP's and is due to an overall cooling of the LSP and a corresponding decrease in global absorption. If this decrease in absorption is greater than the decrease in radiation losses at high mole flux, then thermal efficiency will exhibit a true peak, or optimum value [2].

In summary the highest achieved global absorption was 89.8% with a corresponding thermal efficiency of 78.0% for a 7 kW, f/4, 3.61 atm, 2023 moles/m^{2}s LSP. The highest achieved thermal efficiency at 7 kW was

79.9% with a corresponding global absorption of 89.1% for a f/4, 3.55 atm, 2231 moles/m^{2}s LSP. The highest achieved overall thermal efficiency was 80.2% with a corresponding global absorption of 84.8% for a 4.5 kW, f/4, 4.04 atm, 1823 moles/m^{2}s LSP.

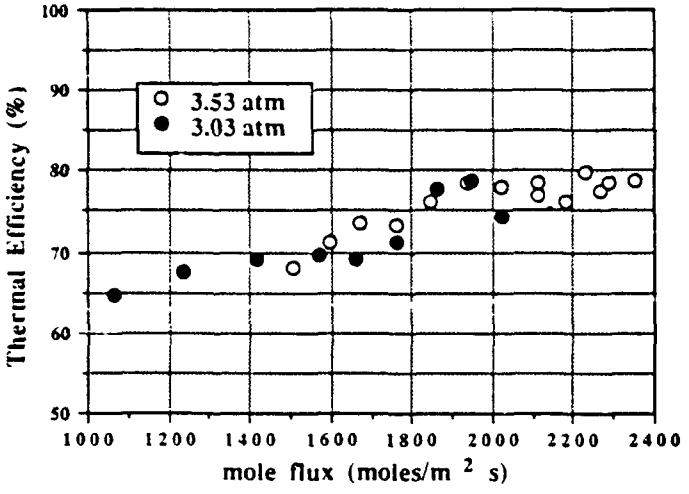

Figure 9 Comparison of thermal efficiency plotted versus mole flux for f/4, 7 kW LSP's at 3.53±0.11 atm and 3.03 ±0.08 atm gas pressure.

Non-LTE Considerations

It is necessary to perform non-Local Thermodynamic Equilibrium (non-LTE) based experiments on laboratory Laser Sustained Plasmas (LSP's) in order to guide the development of an accurate LSP computer simulation. The current LSP model has an inherent LTE assumption in its flow equations and gas property data [4]. The objective of the non-LTE diagnostics is not to verify a condition of non-local thermodynamic equilibrium in an LSP, but to determine this condition specifically in terms of particle number densities and plasma temperatures. From these the extent to which non-LTE conditions affect the plasma performance parameters global absorption and thermal conversion efficiency can be determined. In the event that non-LTE is shown by experiment to play a significant role in the overall performance of LSP's, especially as one attempts to gauge how LSP performance scales with increasing laser power, then the extended computer model will take these effects into account.

A non-LTE plasma will have transport and radiative properties different from an LTE plasma, and this non-LTE is likely to be driven to an ever greater extent as the laser power density increases. This is because the plasma free electrons are heated directly by the laser, and the heavy particles are heated only through subsequent collisional events. Therefore the results of an LTE model would be less and less reliable as power is scaled upward. On the other hand certain non-LTE effects may not be significant as one scales to higher power, especially for a hydrogen LSP at elevated pressure (and correspondingly high electron number density), in which case certain increases in analytical complexity are uncalled for. Therefore it is necessary to perform detailed experiments to determine the types of non-LTE which are important (e.g. kinetic, excitational, or ionizational) to LSP performance in order to incorporate an appropriate amount of complexity into the computer model.

If non-LTE effects do prove to be significant, then a strong research effort will be required to produce a reliable analytical model which includes them. The main benefit of such a model will be the ability to predict LSP behavior as laser power is scaled upward. Optimum operating conditions in terms of global absorption and thermal conversion efficiency and the prediction of thrust and specific impulse will be determined for a given laser power. This type of model is crucial for the design of full-scale laser sustained plasma thrusters.

In this research, diagnostic techniques will be applied which are independent of the LTE assumption. These techniques follow those of Eddy and incorporate both direct spectroscopic measurements and analytic solution techniques [8,9]. Electron number density are determined through either a spectral line broadening measurement or a measurement of continuum emission. The upper level excited state distribution temperature and state populations are determined from a measurement of spectral line intensities. Other relevant parameters such as electron and heavy particle kinetic temperatures, atomic number density, and the total excitation temperature (relating the ground state to the highest excited state), are calculated through an iterative simultaneous solution of the appropriate analytical expressions.

In all previous studies of the types of LSP's considered here (forced convection regime for the laser propulsion application), local laser absorption and radiative emission coefficients were taken to be functions of the plasma electron temperature only, at a given pressure [3,4]. The temperature used was the one found through the use of LTE diagnostics or single temperature modeling. It is a goal of this research to arrive at better values for absorption and emission coefficient based on the measured or calculated value of number densities and temperatures. It is expected that this will lead to a more fundamental understanding of the laser energy conversion process, more accurate determinations of global absorption and thermal conversion efficiency, and a better guideline for an enhanced non-LTE numerical model.

Conclusions

Several conclusions can be drawn from the results just presented.

- It has been reported that at specific impulses of 1300 to 1700 s with a 0.2 to 2 MW laser that a combined efficiency of at least 30% is required to make a laser thruster feasible [10]. This paper presents results for thermal efficiencies of up to 80.2% without the benefit of regenerative techniques and conclusively shows that laser propulsion is a feasible and attractive technology.
- Global absorption increases with input laser power. The power at which 100% absorption is expected depends on the gas pressure.
- LSP's are stable for higher mole fluxes at higher input powers.
- The mole flux for optimal thermal efficiency increases with increasing input power.
- Global absorption at 7 kW increases with gas pressure up to approximately 3.5 atm. Between 3.5 atm and 4 atm no further increases are observed.
- LSP's are stable for higher mole fluxes at higher gas pressures.

• The mole flux for optimal thermal efficiency increases with increasing gas pressure.

• LSP's at f/4 focusing geometry are stable for higher mole fluxes and produce consistently higher global absorption and thermal efficiency than LSP's at f/7 focusing geometry.

• The mole flux for optimal thermal efficiency increases with both increasing input power and gas pressure. This may cause problems in optimization for very high power conditions because the required optimal mole flux may be much higher than the thruster design mole flux. In this case a thruster designed for several lower power LSP's sustained simultaneously may be required.

Acknowledgements

The authors would like to thank Justin Koch of the University of Illinois Materials Engineering Research High Power Laser Laboratory for operating and maintaining the laser which was essential to this work. Also, the guidance of Dr. Thomas Eddy of the Idaho National Engineering Laboratory regarding non-LTE diagnostics has been most helpful.

References

1. Welle, R., Keefer, D., and Peters, C., "Laser-Sustained Plasmas in Forced Argon Convective Flow, Part I: Experimental Studies," AIAA Journal, Vol. 25, Aug. 1987, pp. 1093-1099.

2. Zerkle, D.K., Schwartz, S., Mertogul, A.E., Chen, X., Krier, H., and Mazumder, J., "Laser-Sustained Argon Plasmas for Thermal Rocket Propulsion," Journal of Propulsion and Power, Vol. 6, No. 1, pp. 38-45, January-February 1990.

3. Jeng, S.M., and Keefer, D., "Influence of Laser Beam Geometry and Wavelength on Laser-Sustained Plasmas," AIAA Paper No. 87-1409, June 1987.

4. Schwartz, S., Mertogul, A., Eguiguren, J., Zerkle, D., Chen, X., Krier, H., and Mazumder, J., "Laser-Sustained Gas Plasmas for Application to Rocket Propulsion," AIAA Paper No. 89-2631, AIAA/ASME/SAE/ASEE 25th Joint Propulsion Conference, July 1989.

5. Stallcop, J. R., "Absorption of Laser Radiation in a H-He Plasma. I. Theoretical Calculation of the Absorption Coefficient," Physics of Fluids, Vol. 17 No. 4, p. 751, April 1974.

6. Kline, S. J. and McClintock, F. A., "Describing Uncertainties in Single-Sample Experiments," Mechanical Engineering, p. 3, January 1953.

7. Krier, H., Mazumder, J., Zerkle, D.K., Mertogul, A., Schwartz, S., "Energy Conversion Measurements in Laser-Sustained Argon Plasmas for Application to Rocket Propulsion," Technical Report, Dept. of Mechanical and Industrial Engineering, University of Illinois at Urbana-Champaign, April 1988.

8. Eddy, T. L. and Sedghinasab, A., "The Type and Extent of Non-LTE in Argon Arcs at 0.1-10 Bar," IEEE Transactions on Plasma Science, Vol. 16, No.4, p. 444, 1988.

9. Eddy, T. L., "Low Pressure Plasma Diagnostic Methods," AIAA Paper 89-2830, AIAA/ASME/SAE/ASEE Joint Propulsion Conference, July 1989.

10. Frisbee, R. H., Horvath, J. C., and Sercel, J. C., "Laser Propulsion for the Orbital Transfer Mission," AIAA Paper 85-1224, AIAA/ASME/SAE/ASEE Joint Propulsion Conference, July 1985.